

We are IntechOpen, the world's leading publisher of Open Access books Built by scientists, for scientists

6,900

Open access books available

186,000

International authors and editors

200M

Downloads

Our authors are among the

154

Countries delivered to

TOP 1%

most cited scientists

12.2%

Contributors from top 500 universities



WEB OF SCIENCE™

Selection of our books indexed in the Book Citation Index
in Web of Science™ Core Collection (BKCI)

Interested in publishing with us?
Contact book.department@intechopen.com

Numbers displayed above are based on latest data collected.
For more information visit www.intechopen.com



Synchronous Generator Advanced Control Strategies Simulation

Damir Sumina, Neven Bulić, Marija Mirošević and Mato Mišković
*University of Zagreb/Faculty of Electrical Engineering and Computing,
 University of Rijeka, Faculty of Engineering,
 University of Dubrovnik/Department of Electrical Engineering and Computing
 Croatia*

1. Introduction

During the last two decades, a number of research studies on the design of the excitation controller of synchronous generator have been successfully carried out in order to improve the damping characteristics of a power system over a wide range of operating points and to enhance the dynamic stability of power systems (Kundur, 1994; Noroozi et.al., 2008; Shahgholian, 2010). When load is changing, the operation point of a power system is varied; especially when there is a large disturbance, such as a three-phase short circuit fault condition, there are considerable changes in the operating conditions of the power system. Therefore, it is impossible to obtain optimal operating conditions through a fixed excitation controller. In (Ghandra et.al., 2008; Hsu & Liu, 1987), self-tuning controllers are introduced for improving the damping characteristics of a power system over a wide range of operating conditions. Fuzzy logic controllers (FLCs) constitute knowledge-based systems that include fuzzy rules and fuzzy membership functions to incorporate human knowledge into their knowledge base. Applications in the excitation controller design using the fuzzy set theory have been proposed in (Karnavas & Papadopoulos, 2002; Hiyama et. al., 2006; Hassan et. al., 2001). Most knowledge-based systems rely upon algorithms that are inappropriate to implement and require extensive computational time. Artificial neural networks (ANNs) and their combination with fuzzy logic for excitation control have also been proposed, (Karnavas & Pantos, 2008; Salem et. al., 2000a, Salem et. al., 2000b). A simple structure with only one neuron for voltage control is studied in (Malik et. al., 2002; Salem et. al., 2003). The synergetic control theory (Jiang, 2009) and other nonlinear control techniques, (Akbari & Amooshahi, 2009; Cao et.al., 2004), are also used in the excitation control.

One of the disadvantages of artificial intelligence methods and nonlinear control techniques is the complexity of algorithms required for implementation in a digital control system. For testing of these methods is much more convenient and easier to use software package Matlab Simulink. So, this chapter presents and compares two methods for the excitation control of a synchronous generator which are simulated in Matlab Simulink and compared with conventional control structure. The first method is based on the neural network (NN) which uses the back-propagation (BP) algorithm to update weights on-line. In addition to

the function of voltage control the proposed NN has the function of stabilizing generator oscillations. The second method proposes a fuzzy logic controller (FLC) for voltage control and the stabilization of generator oscillations. The proposed control algorithms with neural networks and a fuzzy controller are tested on a simulation model of synchronous generator weakly connected through transmissions lines to an AC network. The simulations are carried out by step changes in voltage reference.

2. Simulation models

Simulation models of synchronous generator and different control structures are made in Matlab Simulink. The generator is connected over transformer and transmission lines to the AC network (Fig. 1).

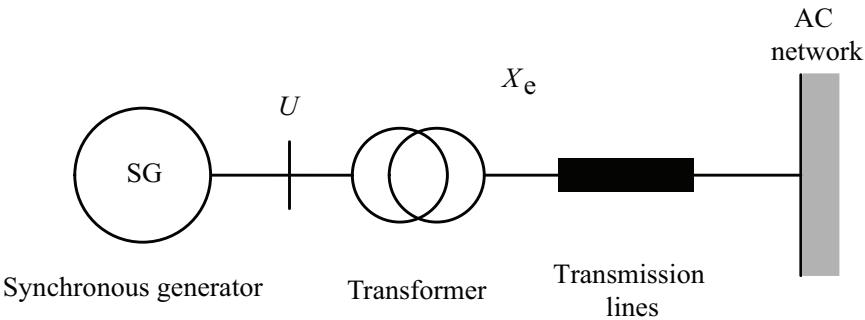


Fig. 1. Synchronous generator connected to AC network

2.1 Simulation model of a synchronous generator

Mathematical model of synchronous generator is represented in *dq* axis form. Based on that it is necessary to perform transformation from *abc* coordinate system to *dq* coordinate system. Assumption is that voltages are symmetrical in all phases and there is only one harmonic of magnetic flux in air gap. Equations are represented in per-unit system and time is absolute.

The synchronous generator under consideration is assumed to have three armature windings, one field winding, and damper windings. One damper winding is located along the direct axis (D) and another is located along the quadrature axis (Q). Accordingly, the basis for the mathematical model of the synchronous generator is a system of voltage equations of the generator in the rotating *dq* coordinate system, where *u*, *i*, *r*, *x* and Ψ denote voltage, current, resistance, reactance and flux, respectively (Kundur, 1994):

$$-u_d = r \cdot i_d + \frac{1}{\omega_s} \cdot \frac{d\Psi_d}{dt} + \omega \cdot \Psi_q$$

(1)

$$-u_q = r \cdot i_q + \frac{1}{\omega_s} \cdot \frac{d\Psi_q}{dt} - \omega \cdot \Psi_d$$

(2)

$$u_f = r_f \cdot i_f + \frac{1}{\omega_s} \cdot \frac{d\Psi_f}{dt}$$

(3)

$$0 = r_D \cdot i_D + \frac{1}{\omega_s} \cdot \frac{d\Psi_D}{dt} \quad (4)$$

$$0 = r_Q \cdot i_Q + \frac{1}{\omega_s} \cdot \frac{d\Psi_Q}{dt} \quad (5)$$

The equations defining the relations between fluxes and currents are:

$$\Psi_d = x_d \cdot i_d + x_{ad} \cdot i_f + x_{dD} \cdot i_D \quad (6)$$

$$\Psi_q = x_q \cdot i_q + x_{qQ} \cdot i_Q \quad (7)$$

$$\Psi_f = x_{ad} \cdot i_d + x_f \cdot i_f + x_{fD} \cdot i_D \quad (8)$$

$$\Psi_D = x_{dD} \cdot i_d + x_{fD} \cdot i_f + x_D \cdot i_D \quad (9)$$

$$\Psi_Q = x_{qQ} \cdot i_q + x_Q \cdot i_Q \quad (10)$$

The motion equations are defined as follows:

$$\frac{d\delta}{dt} = (\omega - 1) \cdot \omega_s \quad (11)$$

$$\frac{d\omega}{dt} = \frac{1}{2H} \cdot (T_m - T_e) \quad (12)$$

where δ is angular position of the rotor, ω is angular velocity of the rotor, ω_s is synchronous speed, H is inertia constant, T_m is mechanical torque, and T_e is electromagnetic torque.

The electromagnetic torque of the generator T_e is determined by equation:

$$T_e = \Psi_q \cdot i_d - \Psi_d \cdot i_q \quad (13)$$

Connection between the synchronous generator and AC network is determined by the following equations:

$$u_d = i_d \cdot r_e + \frac{x_e}{\omega_s} \cdot \frac{di_d}{dt} + \omega \cdot x_e \cdot i_q + u_{sd} \quad (14)$$

$$u_q = i_q \cdot r_e + \frac{x_e}{\omega_s} \cdot \frac{di_q}{dt} - \omega \cdot x_e \cdot i_d + u_{sq} \quad (15)$$

$$u_{sd} = U_m \cdot (-\sin \delta) \quad (16)$$

$$u_{sq} = U_m \cdot \cos \delta \quad (17)$$

transformer and transmission line resistance, x_e is transformer and transmission line reactance, and U_m is AC network voltage. Synchronous generator nominal data and simulation model parameters are given in Table 1.

Terminal voltage	400 V
Phase current	120 A
Power	83 kVA
Frequency	50 Hz
Speed	600 r/min
Power factor	0,8
Excitation voltage	100 V
Excitation current	11.8 A
d-axis synchronous reactance X_d	0.8 p.u.
q-axis synchronous reactance X_q	0.51 p.u.
Inertia constant H	1.3
d-axis transient open-circuit time constant $T_{do'}$	0.55 s
d-axis transient reactance X_d'	0.35 p.u.
d-axis subtransient reactance X_d''	0.15 p.u.
q-axis subtransient reactance X_q''	0.15 p.u.
Short-circuit time constant T_d''	0.054 s
Short-circuit time constant T_q''	0.054 s
Transformer and transmission line resistance r_e	0.05 p.u.
Transformer and transmission line reactance x_e	0.35 p.u.

Table 1. Synchronous generator nominal data and simulation model parameters

2.2 Conventional control structure

Conventional control structure (CCS) for the voltage control of a synchronous generator is shown in Fig. 3. The structure contains a proportional excitation current controller and, subordinate to it, a voltage controller. Simulation model of conventional control structure is shown in Fig. 4.

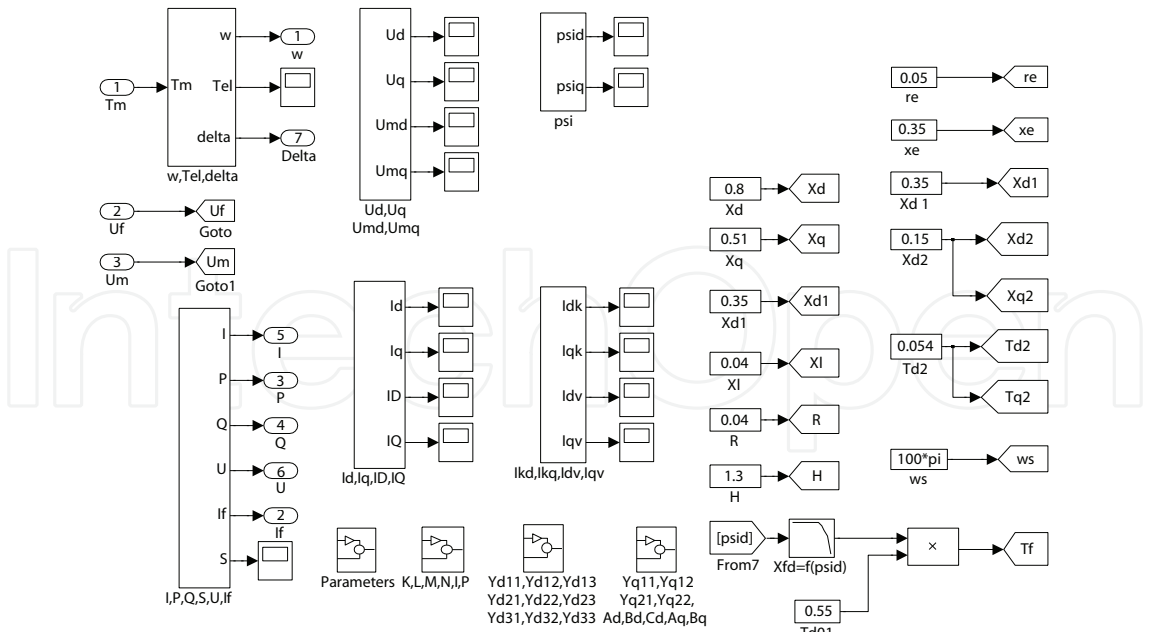


Fig. 2. Simulation model of synchronous generator

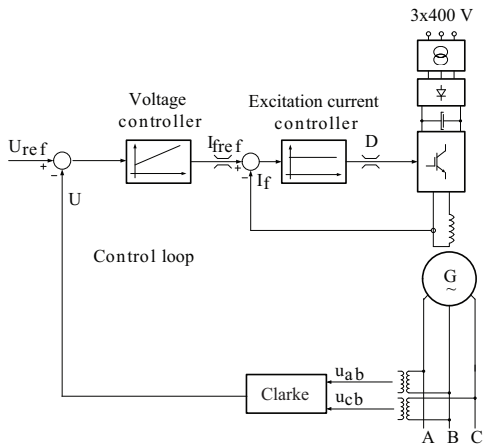


Fig. 3. Conventional control structure

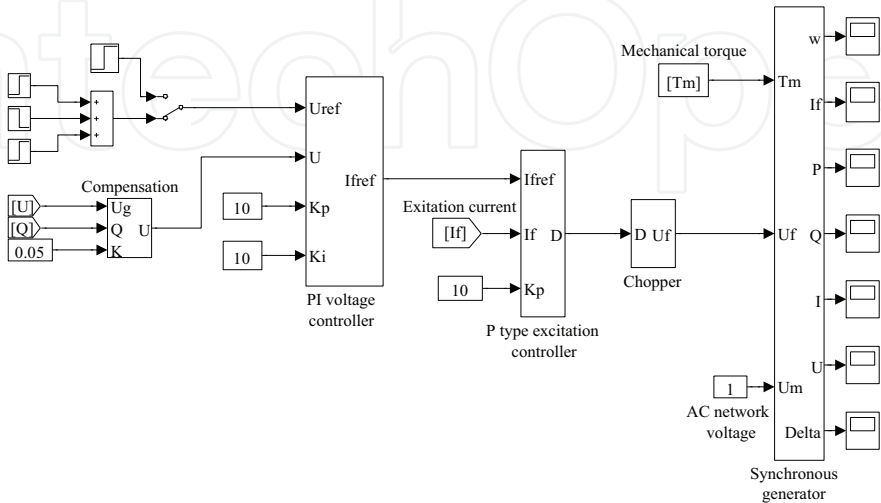


Fig. 4. Simulation model of conventional control structure

For supplying the generator excitation current, an AC/DC converter is simulated. The AC/DC converter includes a three-phase bridge rectifier, a DC link with a detection of DC voltage, a braking resistor, and a DC chopper (Fig. 5).

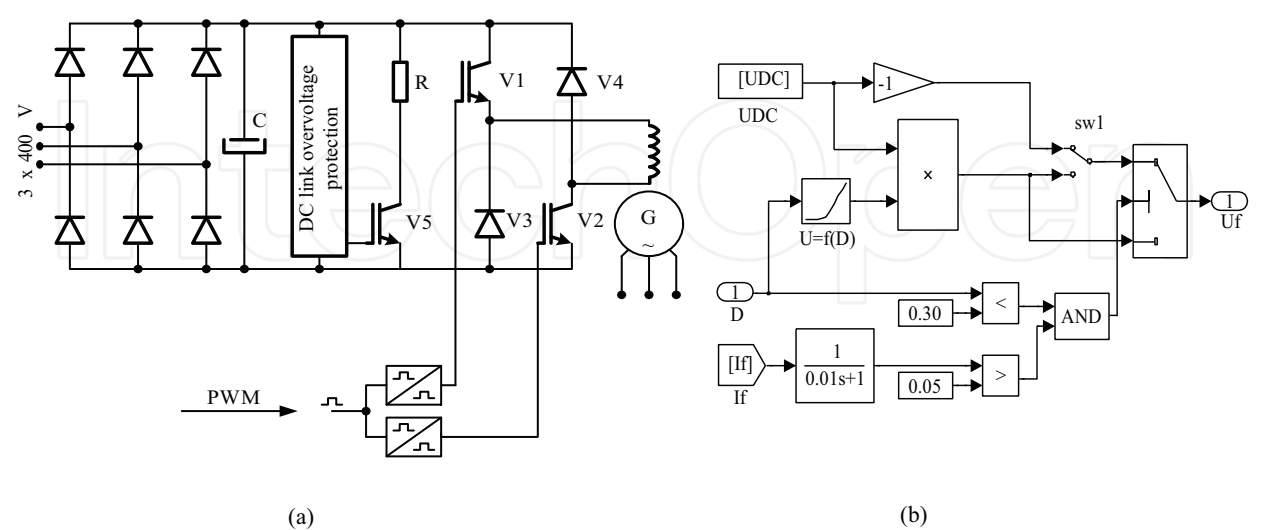


Fig. 5. AC/DC converter for supplying generator excitation current (a) and simulation model (b)

2.3 Neural network based control

The structure of the proposed NN is shown in Fig. 6. The NN has three inputs, six neurons in the hidden layer and one neuron in the output layer. The inputs in this NN are the voltage reference U_{ref} , the terminal voltage U and the previous output from the NN $y(t-1)$. Bringing the previous output to the NN input is a characteristic of dynamic neural networks. The function tansig is used as an activation function for the neurons in the hidden layer and for the neuron in the output layer.

The graphical representation of the tansig function and its derivation is shown in Fig. 7. The numerical representation of the tansig function and its derivation are given as follows (Haykin, 1994):

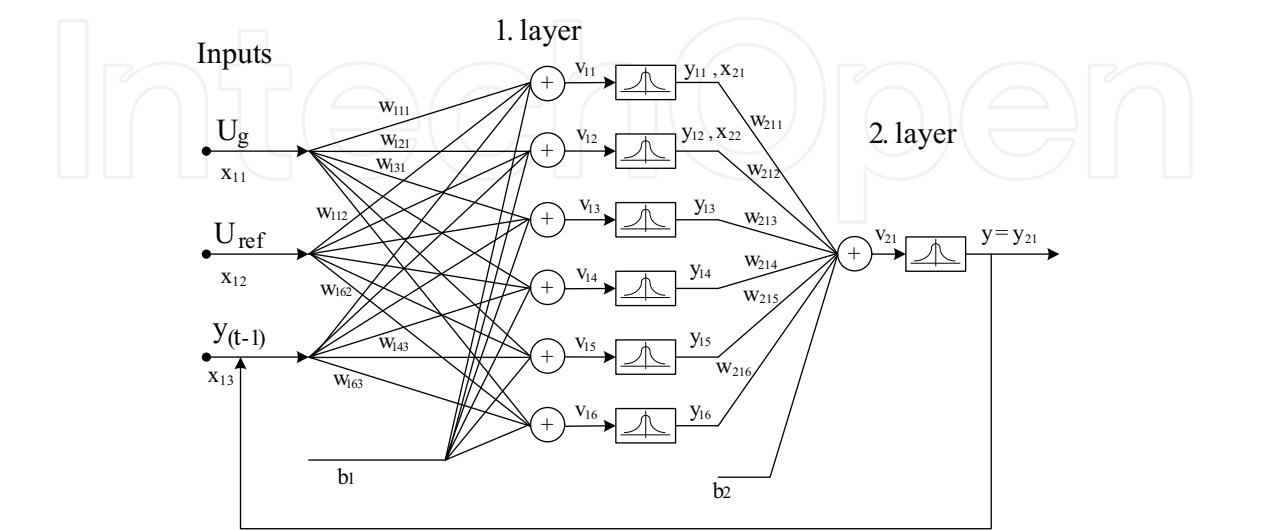


Fig. 6. Structure of the proposed neural network

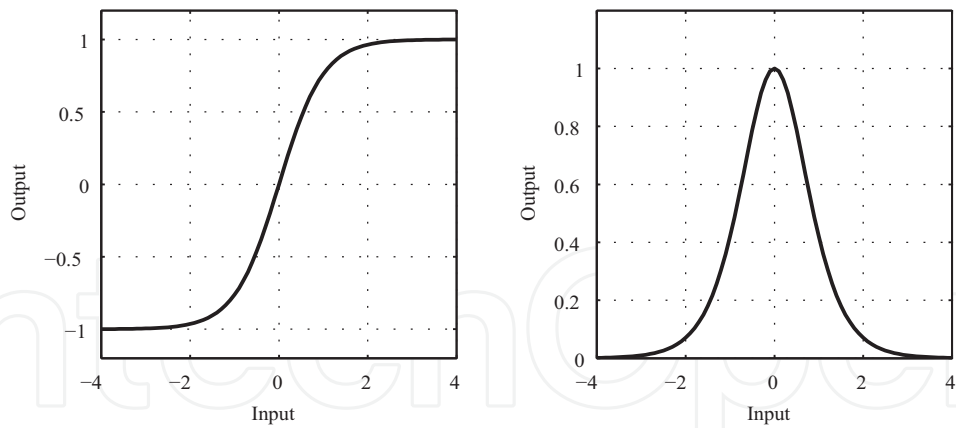


Fig. 7. Tansig activation function and its derivation

$$\psi(v) = \frac{1}{1 + e^{-cv}} - 1$$

(18)

$$\psi'(v) = c \frac{4e^{-2cv}}{(1 + e^{-2cv})^2} = c \cdot (1 - \psi^2)$$

(19)

The NN uses a simple procedure to update weights on-line and there is no need for any off-line training. Also, there is no need for an identifier and/or a reference model. The NN is trained directly in an on-line mode from the inputs and outputs of the generator and there is no need to determine the states of the system. The NN uses a sampled value of the machine quantities to compute the error using a modified error function. This error is back-propagated through the NN to update its weights using the algorithm shown in Fig. 8. When the weights are adjusted, the output of the neural network is calculated.

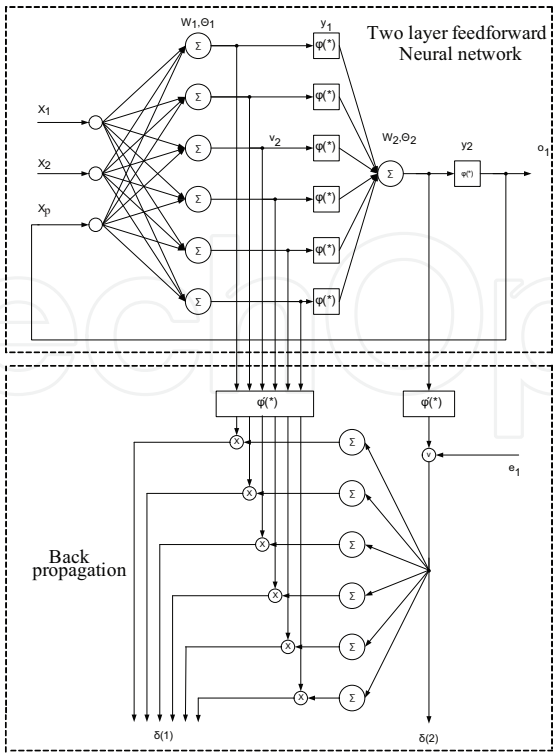


Fig. 8. Back-propagation algorithm

Training of the NN with the BP algorithm is described in (Haykin, 1994). Inputs and outputs of one neuron in the NN can be determined as follows:

$$y_{ki} = \psi \left(\sum_k w_{kij} \cdot x_{kj} + b_1 \right) \quad (20)$$

The BP algorithm is an iterative gradient algorithm designed to minimize the mean square error between the actual output and the NN desired output. This is a recursive algorithm starting at the output neuron and working back to the hidden layer adjusting the weights according to the following equations:

$$w_{kij}(t+1) = w_{kij}(t) + \Delta w_{kij}(t) \quad (21)$$

$$\Delta w_{ji}(n) = \eta \cdot \delta_j(n) \cdot y_i(n) \quad (22)$$

$$\delta_j(n) = e_j(n) \cdot \phi'_j(v_j(n)) \quad (23)$$

The error function commonly used in the BP algorithm can be expressed as:

$$\mathfrak{S} = \frac{1}{2} (t_{ki} - y_{ki})^2 \quad (24)$$

If the neuron is in the output layer, the error function is:

$$\frac{\partial \mathfrak{S}}{\partial y_{ki}} = t_{ki} - y_{ki} \quad (25)$$

If the neuron is in the hidden layer, the error function is recursively calculated as (Haykin, 1994):

$$\frac{\partial \mathfrak{S}}{\partial y_{ki}} = \sum_{p=1}^{n(k+1)} \frac{\partial \mathfrak{S}}{\partial y_{k+1,p}} \cdot \psi'_{k+1,p} \cdot w_{k+1,1,i} \quad (26)$$

If the NN is used for the excitation control of a synchronous generator, it is required that we not only change the weights based only on the error between the output and the desired output but also based on the change of the error as follows:

$$\frac{\partial \mathfrak{S}}{\partial y_{ki}} = (t_{ki} - y_{ki}) - \frac{dy_{ki}}{dt} \quad (27)$$

In this way, the modified error function speeds up the BP algorithm and gives faster convergence. Further, the algorithm becomes appropriate for the on-line learning implementation. The error function for the NN used for voltage control is expressed as:

$$\frac{\partial \mathfrak{S}}{\partial y_{ki}} = K(U_{ref} - U) - k_1 \frac{dU}{dt} \quad (28)$$

In order to perform the power system stabilization, the active power deviation ΔP and the derivation of active power dP/dt are to be imported in the modified error function. The

complete modified error function for the excitation control of a synchronous generator is given as follows:

$$\frac{\partial \mathfrak{Z}}{\partial y_{ki}} = \left[K(U_{ref} - U) - k_1 \frac{dU}{dt} \right] - \left[k_3 (\Delta P) + k_2 \frac{dP}{dt} \right]$$

(29)

The modified error function is divided into two parts. The first part is used for voltage control and the second part for power system stabilization. Parameters K, k₁, k₂ and k₃ are given in Table 2. Simulation model of NN control structure is shown in Fig. 9.

K	2.5
k ₁	0.3
k ₂	0.6
k ₃	0.25

Table 2. Parameters of neural network

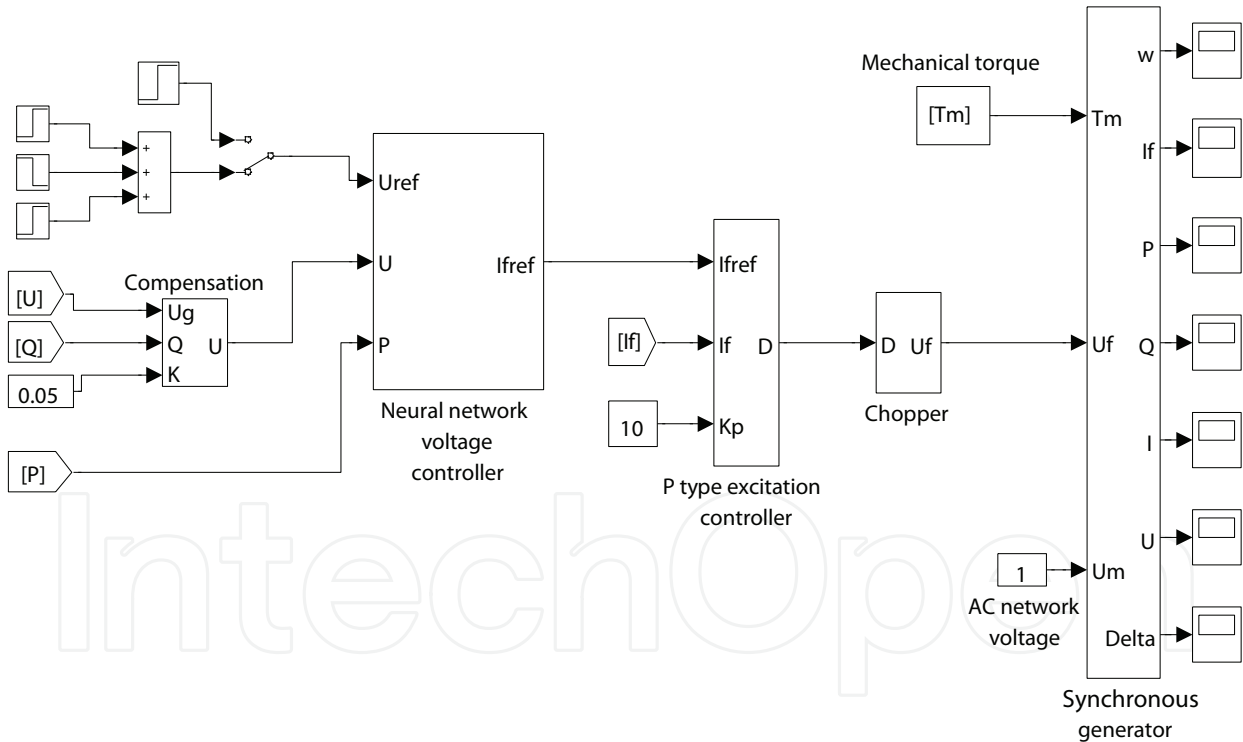


Fig. 9. Simulation model of neural network control structure

Neural network based controller is realized as S-function in Matlab and is called in every simulation step.

2.4 Fuzzy logic controller

The detailed structure of the proposed fuzzy logic controller (FLC) is shown in Fig. 10. The FLC has two control loops. The first one is the voltage control loop with the function of

voltage control and the second one is the damping control loop with the function of a power system stabilizer. A fuzzy polar control scheme is applied to these two control loops.

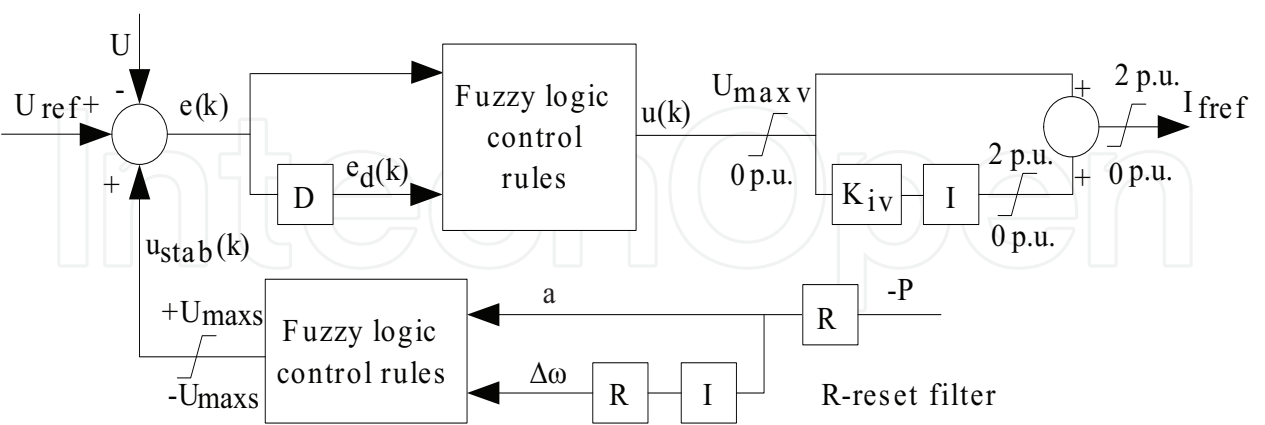


Fig. 10. Structure of the fuzzy logic stabilizing controller

The PD information of the voltage error signal $e(k)$ is utilized to get the voltage state and to determine the reference I_{ref} for the proportional excitation current controller. To eliminate the voltage error, an integral part of the controller with parameter K_{iv} must be added to the output of the controller. The damping control signal u_{stab} is derived from the generator active power P . The signal a is a measure of generator acceleration and the signal $\Delta\omega$ is a measure of generator speed deviation. The signals a and $\Delta\omega$ are derived from the generator active power through filters and the integrator. The damping control signal u_{stab} is added to the input of the voltage control loop.

The fuzzy logic control scheme is applied to the voltage and stabilization control loop (Hiyama et. al., 1996). The generator operating point in the phase plane is given by $p(k)$ for the corresponding control loop (Fig. 11a):

$$p(k) = (X(k), A_s \cdot Y(k)) \tag{30}$$

where $X(k)$ is $e(k)$ and $Y(k)$ is $e_d(k)$ for the voltage control loop, and $X(k)$ is $\Delta\omega(k)$ and $Y(k)$ is $a(k)$ for the stabilization control loop. Parameter A_s is the adjustable scaling factor for $Y(k)$. Polar information, representing the generator operating point, is determined by the radius $D(k)$ and the phase angle $\Theta(k)$:

$$D(k) = \sqrt{X(k)^2 + (A_s \cdot Y(k))^2} \tag{31}$$

$$\Theta(k) = \arctg\left(\frac{A_s \cdot Y(k)}{X(k)}\right) \tag{32}$$

The phase plane is divided into sectors A and B defined by using two angle membership functions $N(\Theta(k))$ and $P(\Theta(k))$ (Fig. 11b).

The principles of the fuzzy control scheme and the selection of the membership functions are described in (Hiyama et. al., 1996). By using the membership functions $N(\Theta(k))$ and $P(\Theta(k))$ the output control signals $u(k)$ and $u_{\text{stab}}(k)$ for each control loop are given as follows:

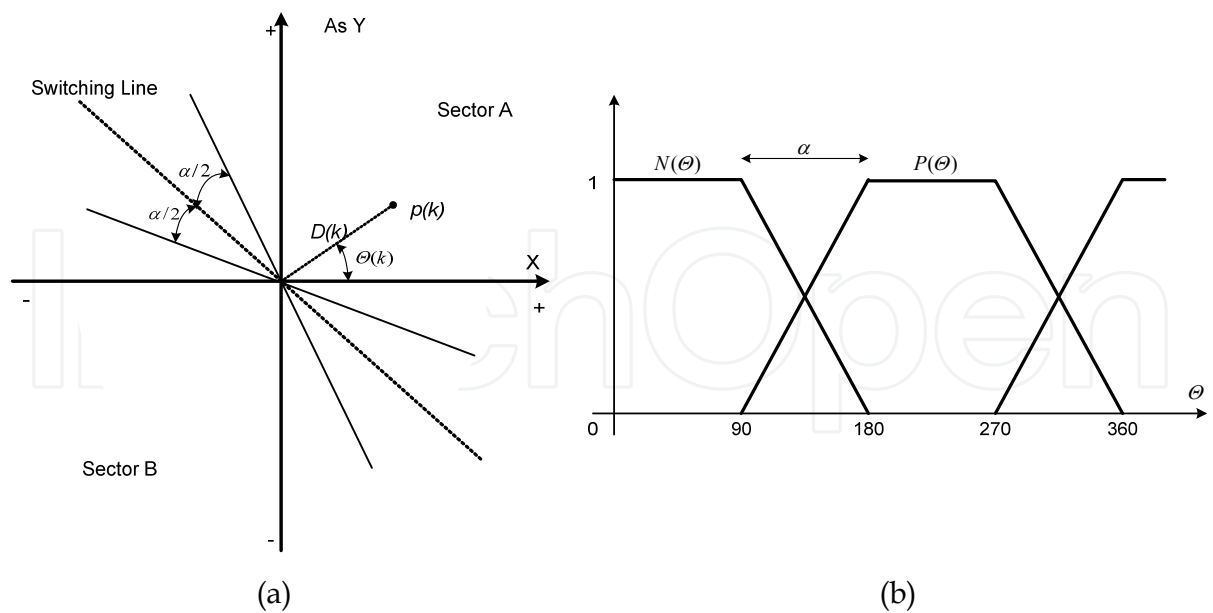


Fig. 11. Phase plane (a) and angle membership functions (b)

$$u(k)=\frac{N(\Theta(k))-P(\Theta(k))}{N(\Theta(k))+P(\Theta(k))}\cdot G(k)\cdot U_{\max v} \tag{33}$$

$$u_{\text{stab}}(k)=\frac{N(\Theta(k))-P(\Theta(k))}{N(\Theta(k))+P(\Theta(k))}\cdot G(k)\cdot U_{\max s} \tag{34}$$

The radius membership function $G(k)$ is given by:

$$\begin{aligned} G(k) &= D(k) / D_r \text{ for } D(k) \leq D_r \\ G(k) &= 1 \text{ for } D(k) > D_r \end{aligned} \tag{35}$$

Simulation models of the voltage control loop, stabilization control loop and fuzzy logic control structure are presented on the Figs. 12, 13, and 14, respectively. Parameters A_s , D_r and α for the voltage control loop and the damping control loop are given in Tables 3 and 4.

A_s	0.1
D_r	1
K_{iv}	10
$U_{\max v}$	2 p.u.
α	90°

Table 3. FLC parameters for voltage control loop

A_s	0.01
D_r	0.01
$U_{\max s}$	0.1 p.u.
α	90°

Table 4. FLC parameters for damping control loop

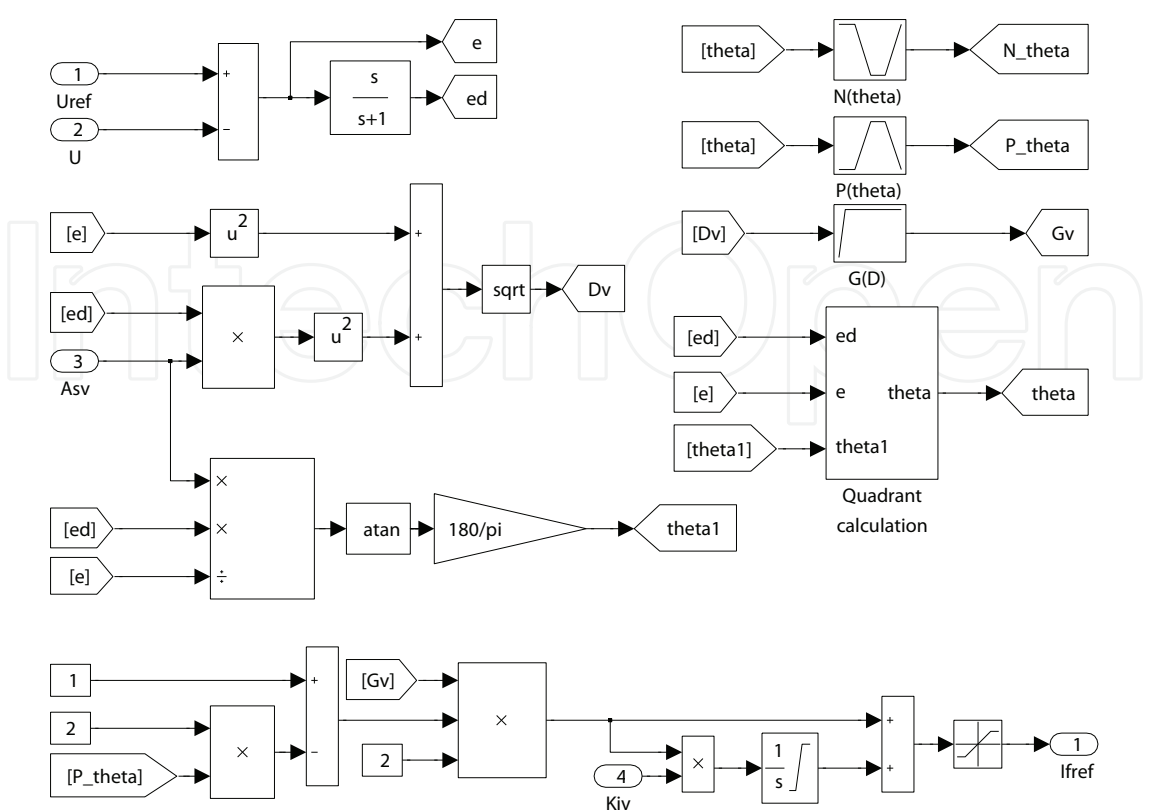


Fig. 12. Simulation model of voltage control loop

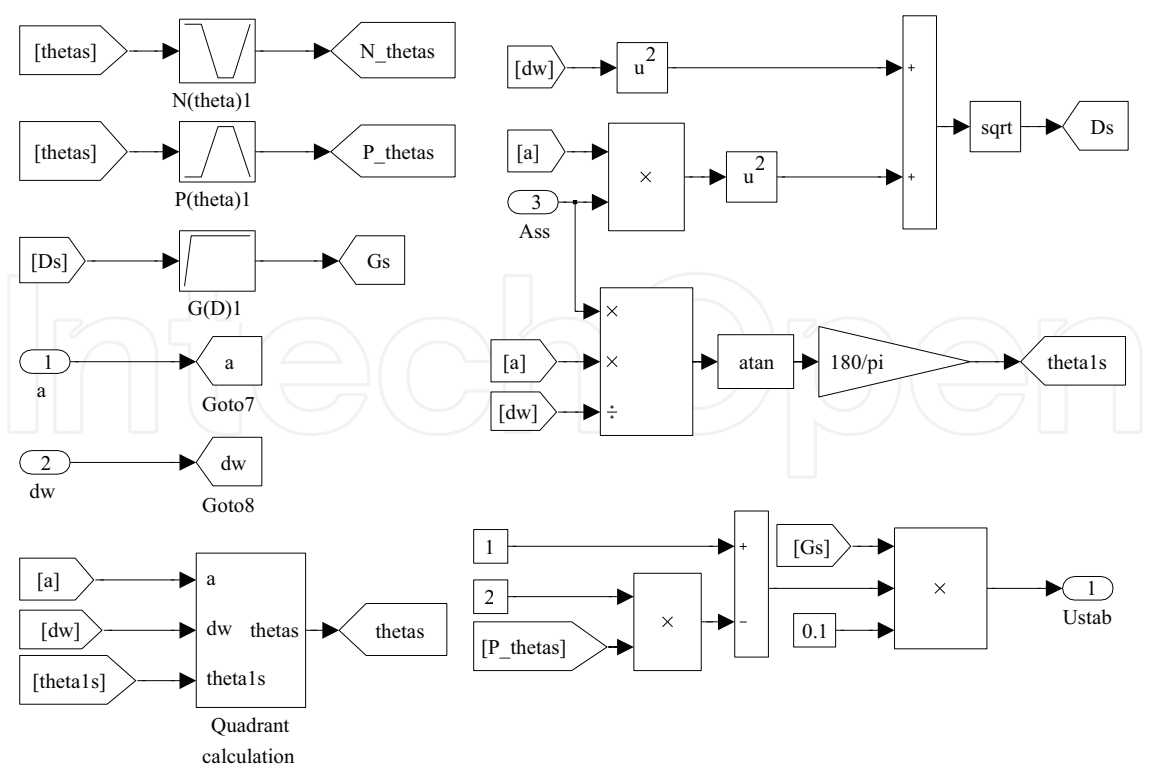


Fig. 13. Simulation model of stabilization control loop

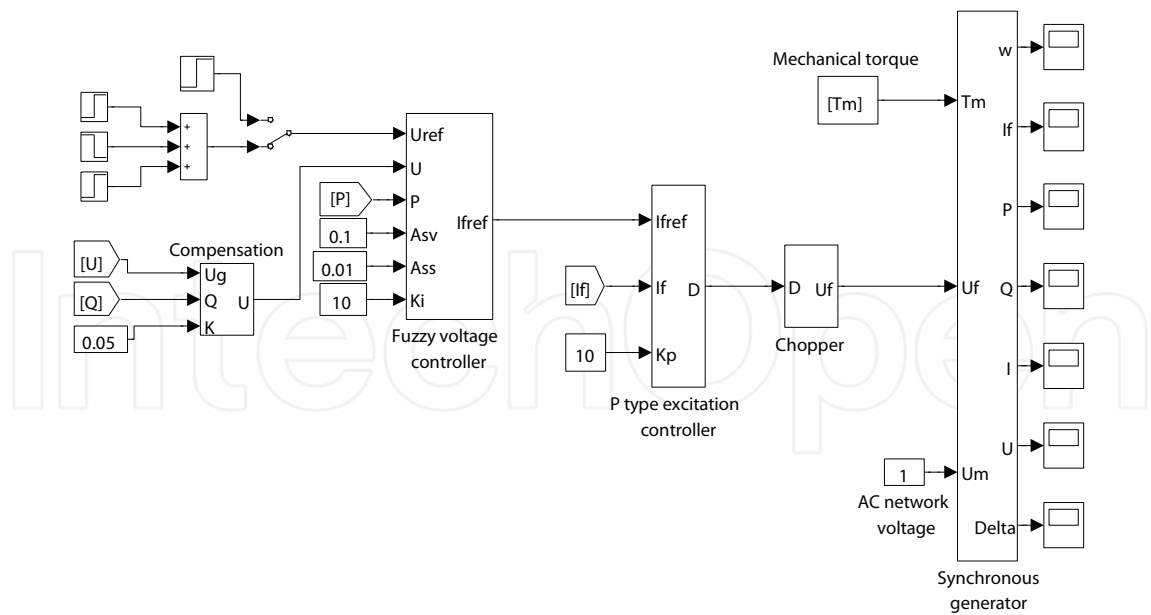


Fig. 14. Simulation model of fuzzy logic control structure

3. Simulation results

In order to verify the performance of the proposed control structures several simulations were carried out. In these experiments, voltage reference is changed in 0.1 s from 1 p.u. to 0.9 p.u. or 1.1 p.u. and in 1 s back to 1 p.u. at a constant generator active power. For the quality analysis of the active power oscillations two numerical criteria are used: the integral of absolute error (IAE) and the integral of absolute error derivative (IAED). If the response is better, the amount of criteria is smaller. Fig. 15 presents active power responses for step changes in voltage reference from 1 p.u. to 0.9 p.u. and back to 1 p.u. at an active power of 0.5 p.u. The numerical criteria of the responses in Fig. 15 are given in Table 5.

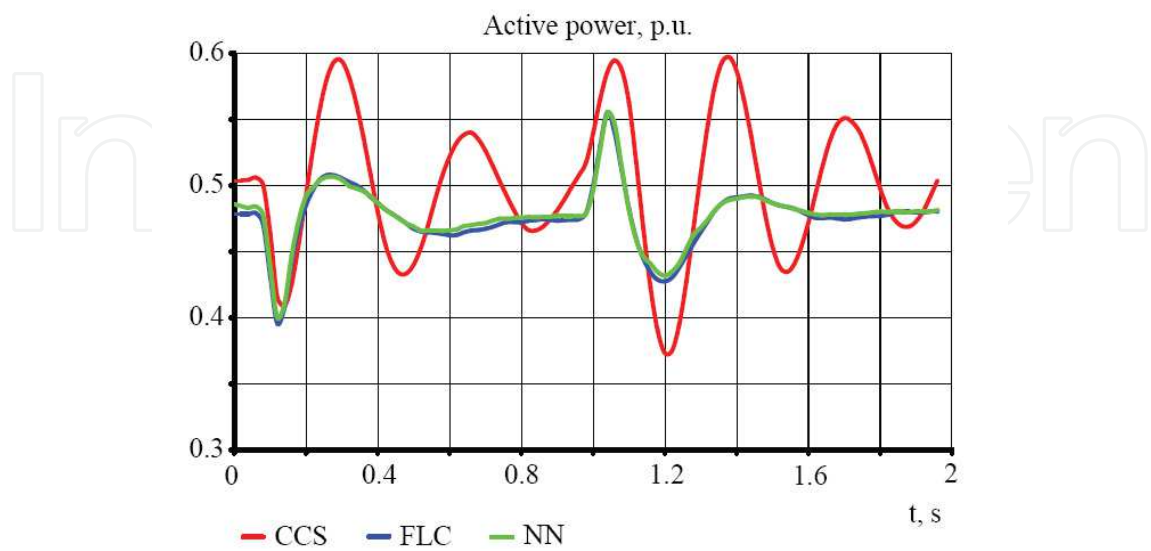


Fig. 15. Active power responses for step changes in voltage reference 1 p.u.-0.9 p.u.-1 p.u. at an active power of 0.5 p.u.

	IAE	IAED
CCS	0.389	0.279
FLC	0.255	0.097
NN	0.235	0.090

Table 5. Numerical criteria for step changes in voltage reference 1 p.u.-0.9 p.u.-1 p.u. at an active power of 0.5 p.u.

Fig. 16 shows active power responses for step changes in voltage reference from 1 p.u. to 1.1 p.u. and back to 1 p.u. at an active power of 0.5 p.u. The numerical criteria of the responses in Fig. 16 are given in Table 6.

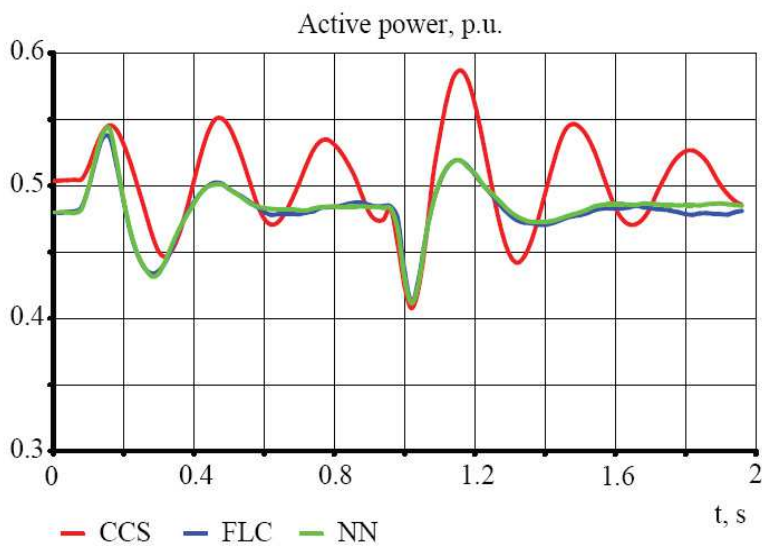


Fig. 16. Active power responses for step changes in voltage reference 1 p.u.-1.1 p.u.-1 p.u. at an active power of 0.5 p.u.

	IAE	IAED
CCS	0.264	0.196
FLC	0.202	0.092
NN	0.192	0.091

Table 6. Numerical criteria for step changes in voltage reference 1 p.u.-1.1 p.u.-1 p.u. at an active power of 0.5 p.u.

Fig. 17 presents active power responses for step changes in voltage reference from 1 p.u. to 0.9 p.u. and back to 1 p.u. at an active power of 0.8 p.u. The numerical criteria of the responses in Fig. 17 are given in Table 7.

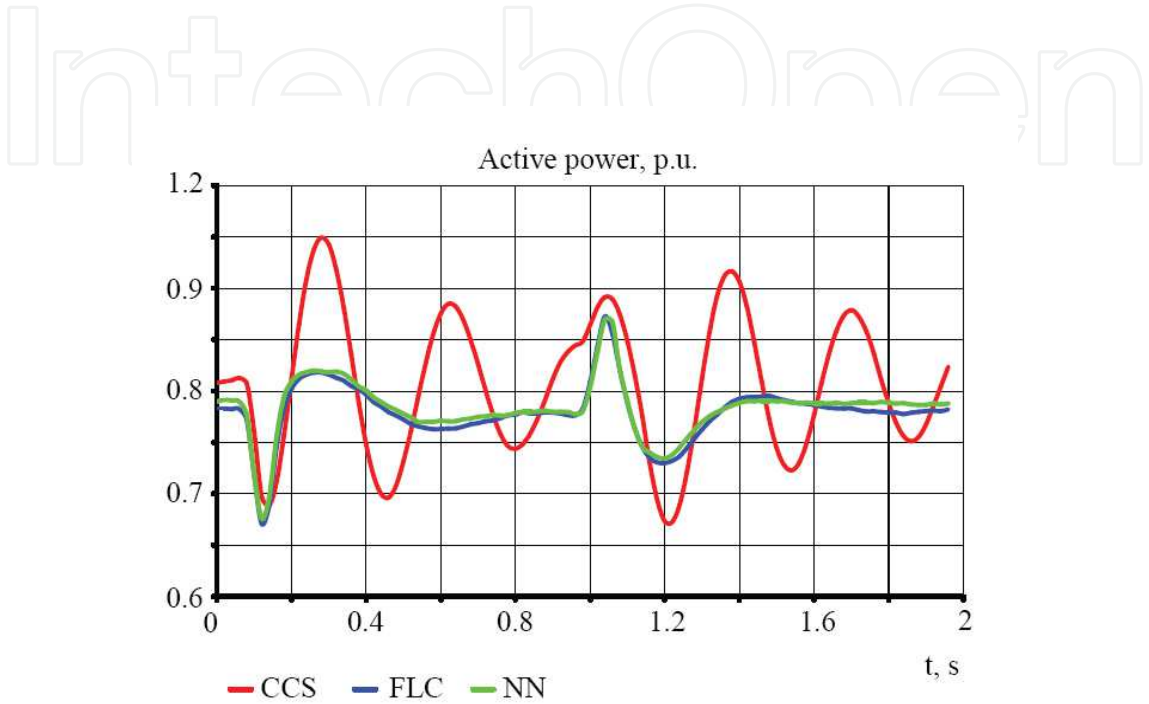


Fig. 17. Active power responses for step changes in voltage reference 1 p.u.-0.9 p.u.-1 p.u. at an active power of 0.8 p.u.

	IAE	IAED
CCS	0.52	0.373
FLC	0.248	0.114
NN	0.219	0.106

Table 7. Numerical criteria for step changes in voltage reference 1 p.u.-0.9 p.u.-1 p.u. at an active power of 0.8 p.u.

Fig. 18 shows active power responses for step changes in voltage reference from 1 p.u. to 1.1 p.u. and back to 1 p.u. at an active power of 0.8 p.u. The numerical criteria of the responses in Fig. 18 are given in Table 8.

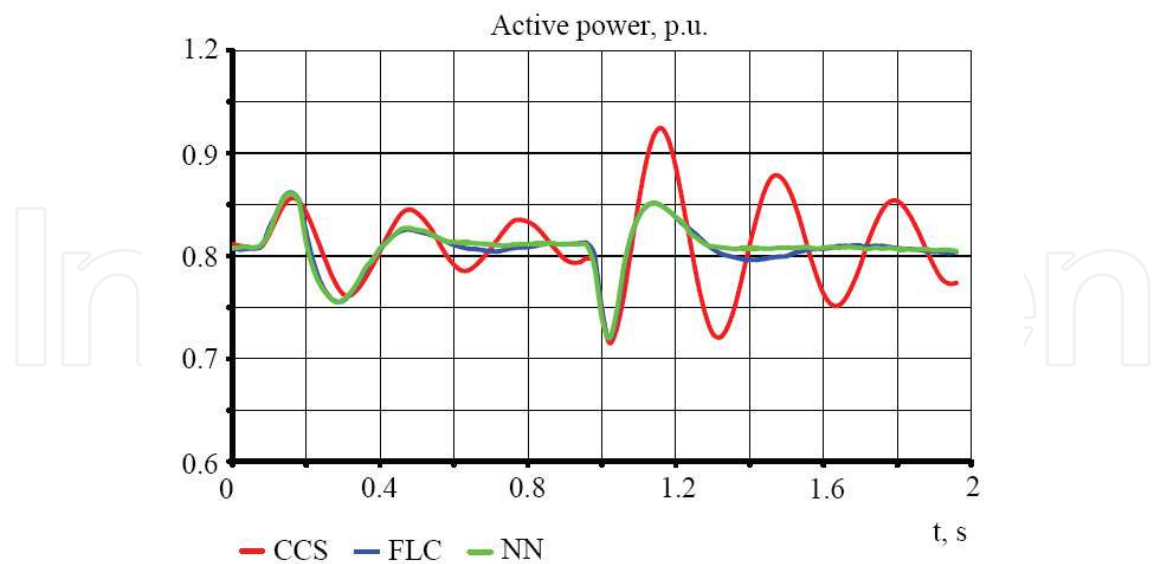


Fig. 18. Active power responses for step changes in voltage reference 1 p.u.-1.1 p.u.-1 p.u. at an active power of 0.8 p.u.

	IAE	IAED
CCS	0.312	0.234
FLC	0.130	0.097
NN	0.119	0.090

Table 8. Numerical criteria for step changes in voltage reference 1 p.u.-1.1 p.u.-1 p.u. at an active power of 0.8 p.u.

Based on the numerical criteria it can be concluded that the neural network-based controller with stabilization effect in the criteria function has two to three percent better damping of oscillations than the fuzzy logic controller.

4. Conclusion

Three different structures for the excitation control of a synchronous generator were simulated in Matlab Simulink: the first structure is a conventional control structure which includes a PI voltage controller, while the second structure includes a fuzzy logic controller, and the third structure includes a neural network-based voltage controller. Performances of the proposed algorithms were tested for step changes in voltage reference in the excitation system of a synchronous generator, which was connected to an AC network through a transformer and a transmission line. For the performance analysis of the proposed control structures two numerical criteria were used: the integral of absolute error and the integral of absolute error derivative. In the comparison with the PI voltage controller neural network-based controller and the fuzzy logic controller show a significant damping of oscillations. It is important to emphasize that

the stabilizer was not used in the conventional control structure, which would definitely reduce the difference between the conventional and the proposed control structures.

The simulation results show justification for the use of the advanced control structure based on neural networks and fuzzy logic in the excitation control system of a synchronous generator. Also, using the software package Matlab Simulink allows users to easily test the proposed algorithms.

5. References

- Akbari, S., & Karim Amooshahi, M. (2009). Power System Stabilizer Design Using Evolutionary Algorithms, *International Review of Electrical Engineering*, 4, 5, (October 2009), pp. 925-931.
- Cao, Y., Jiang, L., Cheng, S., Chen, D., Malik, O.P., & Hope, G.S. (1994). A nonlinear variable structure stabilizer for power system stability, *IEEE Transactions on Energy Conversion*, 9, 3, (1994), pp. 489-495.
- Ghandra, A., Malik, & O. P., Hope, G.S. (1988). A self-tuning controller for the control of multi-machine power systems, *IEEE Trans. On Power Syst.*, 3, 3, (August 1988), pp. 1065-1071.
- Hassan, M.A., Malik, O.P., & Hope, G.S. (1991). A Fuzzy Logic Based Stabilizer for a Synchronous Machine, *IEEE Trans. Energy Conversion*, 6, 3, (1991), pp. 407-413.
- Haykin, S. (1994). *Neural Networks: A Comprehensive Foundation*, IEEE Press
- Hiyama T., Oniki S., & Nagashima H. (1996). Evaluation of advanced fuzzy logic PSS on analog network simulator and actual installation on hydro generators, *IEEE Trans. on Energy Conversion*, 11, 1, (1996), pp. 125-131.
- Hsu, Y.Y., & Liou, K.L. (1987). Design of self-tuning PID power system stabilizers for synchronous generators, *IEEE Trans. on Energy Conversion*, 2, 3, (1987), pp. 343-348.
- Jiang, Z. (2009). Design of a nonlinear power system stabilizer using synergetic control theory, *Electric Power Systems Research*, 79, 6, (2009), pp. 855-862.
- Karnavas, Y.L., & Pantos, S. (2008). Performance evaluation of neural networks for μ C based excitation control of a synchronous generator, *Proceedings of 18th International Conference on Electrical Machines ICEM 2008*, Portugal, September 2008.
- Karnavas, Y.L., & Papadopoulos, D. P. (2002). AGC for autonomous power system using combined intelligent techniques, *Electric Power Systems Research*, 62, 3, (July 2002), pp. 225-239.
- Kundur, P. (1994). *Power System Stability and Control*, McGraw-Hill
- Malik, O.P., Salem, M.M., Zaki, A.M., Mahgoub, O.A., & Abu El-Zahab, E. (2002). Experimental studies with simple neuro-controller based excitation controller, *IEE Proceedings Generation, Transmission and Distribution*, 149, 1, (2002), pp. 108-113.
- Noroozi, N., Khaki, B., & Seifi, A. (2008). Chaotic Oscillations Damping in Power System by Finite Time Control, *International Review of Electrical Engineering*, 3, 6, (December 2008), pp. 1032-1038.

- Salem, M.M., Malik, O.P., Zaki, A.M., Mahgoub, O.A., & Abu El-Zahab, E. (2003). Simple neuro-controller with modified error function for a synchronous generator, *Electrical Power and Energy Systems*, 25, (2003), pp. 759-771.
- Salem, M.M., Zaki, A.M., Mahgoub, O.A., Abu El-Zahab, E., & Malik, O.P. (2000a). Studies on Multi-Machine Power System With a Neural Network Based Excitation Controller, *Proceedings of Power Engineering Society Summer Meeting*, 2000.
- Salem, M.M., Zaki, A.M., Mahgoub, O.A., Abu El-Zahab, E., & Malik, O.P. (2000b). Experimental Veification of Generating Unit Excitation Neuro-Controller, *Proceedings of IEEE Power Engineering Society Winter Meeting*, 2000.
- Shahgholian, G. (2010). Development of State Space Model and Control of the STATCOM for Improvement of Damping in a Single-Machine Infinite-Bus, *International Review of Electrical Engineering*, 5, 1, (February 2010), pp. 1367-1375.

IntechOpen



MATLAB - A Ubiquitous Tool for the Practical Engineer

Edited by Prof. Clara Ionescu

ISBN 978-953-307-907-3

Hard cover, 564 pages

Publisher InTech

Published online 13, October, 2011

Published in print edition October, 2011

A well-known statement says that the PID controller is the “bread and butter” of the control engineer. This is indeed true, from a scientific standpoint. However, nowadays, in the era of computer science, when the paper and pencil have been replaced by the keyboard and the display of computers, one may equally say that MATLAB is the “bread” in the above statement. MATLAB has become a de facto tool for the modern system engineer. This book is written for both engineering students, as well as for practicing engineers. The wide range of applications in which MATLAB is the working framework, shows that it is a powerful, comprehensive and easy-to-use environment for performing technical computations. The book includes various excellent applications in which MATLAB is employed: from pure algebraic computations to data acquisition in real-life experiments, from control strategies to image processing algorithms, from graphical user interface design for educational purposes to Simulink embedded systems.

How to reference

In order to correctly reference this scholarly work, feel free to copy and paste the following:

Damir Sumina, Neven Bulić, Marija Mirošević and Mato Mišković (2011). Synchronous Generator Advanced Control Strategies Simulation, MATLAB - A Ubiquitous Tool for the Practical Engineer, Prof. Clara Ionescu (Ed.), ISBN: 978-953-307-907-3, InTech, Available from: <http://www.intechopen.com/books/matlab-a-ubiquitous-tool-for-the-practical-engineer/synchronous-generator-advanced-control-strategies-simulation>

INTECH
open science | open minds

InTech Europe

University Campus STeP Ri
Slavka Krautzeka 83/A
51000 Rijeka, Croatia
Phone: +385 (51) 770 447
Fax: +385 (51) 686 166
www.intechopen.com

InTech China

Unit 405, Office Block, Hotel Equatorial Shanghai
No.65, Yan An Road (West), Shanghai, 200040, China
中国上海市延安西路65号上海国际贵都大饭店办公楼405单元
Phone: +86-21-62489820
Fax: +86-21-62489821

© 2011 The Author(s). Licensee IntechOpen. This is an open access article distributed under the terms of the [Creative Commons Attribution 3.0 License](https://creativecommons.org/licenses/by/3.0/), which permits unrestricted use, distribution, and reproduction in any medium, provided the original work is properly cited.

IntechOpen

IntechOpen